Journal of Statistical Physics, Vol. 45, Nos. 5/6, 1986

Microstructure Characterization and Bulk Properties of Disordered Two-Phase Media

S. Torquato[1]

Received March 5, 1986; revision received August 20, 1986

A general formalism is developed to statistically characterize the microstructure of porous and other composite media composed of inclusions (particles) distributed throughout a matrix phase (which, in the case of porous media, is the void phase). This is accomplished by introducing a new and general n-point distribution function H_n and by deriving two series representations of it in terms of the probability density functions that characterize the configuration of particles; quantities that, in principle, are known for the ensemble under consideration. In the special case of an equilibrium ensemble, these two equivalent but topologically different series for the H_n are generalizations of the Kirkwood–Salsburg and Mayer hierarchies of liquid-state theory for a special mixture of particles described in the text. This methodology provides a means of calculating any class of correlation functions that have arisen in rigorous bounds on transport properties (e.g., conductivity and fluid permeability) and mechanical properties (e.g., elastic moduli) for nontrivial models of two-phase disordered media. Asymptotic and bounding properties of the general function H_n are described. To illustrate the use of the formalism, some new results are presented for the H_n and it is shown how such information is employed to compute bounds on bulk properties for models of fully penetrable (i.e., randomly centered) spheres, totally impenetrable spheres, and spheres distributed with arbitrary degree of impenetrability. Among other results, bounds are computed on the fluid permeability, for assemblages of impenetrable as well as penetrable spheres, with heretofore unattained accuracy.

KEY WORDS: Disordered media, composite and porous materials; n-point distribution functions; microstructure; Kirkwood–Salsburg equations; Mayer equations, scaled-particle theory; effective conductivity; elastic moduli; fluid permeability; liquids.

---

[1] Departments of Mechanical and Aerospace Engineering and of Chemical Engineering, North Carolina State University, Raleigh, North Carolina 27695-7910.

0022-4715/86/1200-0843$05.00/0

1. INTRODUCTION

The quantitative characterization of the microstructure of disordered media is an important problem in both the physical and natural sciences. In many man-made and natural instances, the disordered medium is composed of two phases such that one of the phases consists of discrete inclusions (particles) distributed throughout a matrix phase according to some probability density function. Examples of such disordered two-phase media include composite materials, suspensions, porous media, and biological membranes, to mention but a few. In the case of porous media, the matrix phase represents the void or pore phase.

Two-phase composite media can be characterized by the n-point correlation functions, which give the probability of simultaneously finding n points with positions $\mathbf{x}_1, \mathbf{x}_2, ..., \mathbf{x}_n$ in one of the phases, say phase 1. This quantity is denoted by $S_n(\mathbf{x}^n)$, where $\mathbf{x}^n$ stands for the set $\{\mathbf{x}_1, ..., \mathbf{x}_n\}$. For statistically homogeneous media S_1 is simply the volume fraction of phase 1. These correlation functions are fundamental to the study of the conductivity (or, because of mathematical analogy, dielectric constant and diffusion coefficient) of suspensions,(1–4) fluid permeability(5,6) of porous media, rate constants associated with diffusion-controlled reactions in porous media,(7) and the elastic moduli of composite materials.(8–10) For a statistically inhomogeneous two-phase medium consisting of identical particles dispersed throughout a matrix phase such that the location of each inclusion is fully specified by a position vector (e.g., spheres, parallel cubes, etc.), the S_n may be systematically represented in terms of the n-particle probability density functions ρ_n.(11,12) [The $\rho_n(\mathbf{r}^n)$ characterizes the probability of simultaneously finding a particle centered in volume element $d\mathbf{r}_1$, another particle centered in volume element $d\mathbf{r}_2$, etc.] For brevity, we shall henceforth state that $\rho_n(\mathbf{r}^n)$ characterizes the probability of finding any n particles with configuration $\mathbf{r}^n$. Lower order n-point "matrix" probability functions S_n, such as $S_1 = \phi$ (the matrix volume fraction), S_2 and S_3, have been evaluated for various distributions of spheres in a matrix.(13–15)

For the case of spheres distributed throughout a matrix, Torquato(16) has derived so-called nth-order cluster bounds on the effective conductivity, which depend upon the microstructure through the set of statistical quantities $G_0^{(1)}$, $G_1^{(1)}, ..., G_{2n}^{(1)}$. The $G_n^{(1)}(\mathbf{x}_1; \mathbf{r}^n)$, which have been termed point/n-particle distribution functions,(16) characterize the probability of finding a point at $\mathbf{x}_1$ in the matrix phase and a configuration of n spheres with coordinates $\mathbf{r}^n$, respectively. As successively more statistical information is included, the bounds become progressively tighter.

Other important descriptors of the microstructure of disordered two-phase media involve information about the two-phase interface. Such quantities arise in transport problems in which the interfacial surface plays a major role in determining the effective transport properties, e.g., the rate constant associated with diffusion-controlled reactions and the fluid permeability of porous media. We shall refer to statistical quantities that involve the two-phase interface as surface correlation functions. The simplest of such quantitites is the specific surface s (expected interface area per unit volume), a one-point correlation function. Doi(17) has obtained bounds on bulk properties associated with diffusion-controlled reactions and flow in porous media in terms of not only ϕ, s, and S_2, but of a surface-matrix $F_{\rm sm}(\mathbf{x}_1, \mathbf{x}_2)$ and a surface–surface correlation function $F_{\rm ss}(\mathbf{x}_1, \mathbf{x}_2)$. The $F_{\rm sm}$ and $F_{\rm ss}$ give the correlations associated with finding a point on the two-phase interface and another point in the matrix phase or on the interface, respectively. Higher order extensions of Doi's bounds involve successively higher order surface correlation functions, such as $F_{\rm sss}$, $F_{\rm ssm}$, $F_{\rm smm}$, etc. For a bed of spheres, Weissberg and Prager(18) have derived a bound on the permeability of such a system that depends upon ϕ, s, a quantity closely related to a surface–particle correlation function $F_{\rm sp}$ (which gives the correlation associated with finding a point on the particle–matrix interface and the center of a sphere in some volume element), $G_1^{(1)}(\mathbf{x}_1; \mathbf{r}_1)$, and $G_2^{(1)}(\mathbf{x}_1; \mathbf{r}_1, \mathbf{r}_2)$. The Weissberg–Prager bound may be extended to include higher-order generalizations of these functions. (The $G_n^{(1)}$ obviously do not explicitly involve information about the interface, but, as shall be shown, are related to the other surface correlation functions described above.) A systematic means of representing and calculating surface correlation functions has heretofore been lacking and hence application of bounds that depend upon such information has been very limited.(19)

The purpose of this paper is to develop a general framework from which we may derive all of the aforementioned correlation functions (i.e., the S_n, $G_n^{(1)}$, $F_{\rm ss}$, $F_{\rm sm}$, $F_{\rm sp}$, $F_{\rm sss}$, $F_{\rm ssm}$, etc.), which in the past have been treated separately, and their generalizations described below. This is done by introducing a very general n-point distribution function H_n and by obtaining series representations of it, from which we may calculate various sets of distribution functions for nontrivial models of two-phase media. This analysis will enable one to study the relationship between the various sets of correlation functions that arise in bounds on effective properties and thus will aid in establishing the connection between the different bounds (e.g., finding the connection between conductivity bounds of Beran(2) and of Torquato,(16) which incorporate the sets S_1, S_2, S_3, and $G_0^{(1)}$, $G_1^{(1)}$, $G_2^{(1)}$, respectively). Moreover, the formalism given here will enable one to calculate bounds on bulk properties of two-phase media with very high accuracy. Finally, we note that the H_n also can be used to characterize the structure of liquids.

In Section 2 we define certain n-point distribution functions G_n and H_n in terms of characteristic functions. It is shown that all of the statistical quantities described above are special cases of the functions G_n and H_n; H_n being the more general of the two. Some properties of the G_n and H_n that follow from their definitions are described. In Section 3 we derive two equivalent but topologically different series representations of both G_n and H_n for general ensembles. For the special case of an equilibrium ensemble, the two series for the H_n are generalizations of the Kirkwood–Salsburg(20) and Mayer(21) hierarchies for a certain equilibrium mixture of particles. The nature of these series enables us to obtain successive rigorous upper and lower bounds on the G_n and H_n. In Section 4 we illustrate the applicability of this formalism by obtaining and presenting new results for the H_n and for bounds on transport properties that depend upon the H_n, for models of fully penetrable, totally impenetrable, and partially penetrable spheres. Among other results, we compute bounds on the permeability, for beds of impenetrable as well as partially penetrable spheres, with heretofore unattained accuracy.

2. GENERAL *n*-POINT DISTRIBUTION FUNCTIONS

2.1. Definitions in Terms of Characteristic Functions

The notion that the n-point matrix probability function S_n is trivially related to the probability density associated with finding a particular configuration of n spherical "solute" or "test" particles of zero radius in a mixture consisting of n such solute particles and N spherical "solvent" particles of radius R (where $n \ll N$) has been profitably exploited by Torquato and Stell(12) to obtain series representations of the S_n.

Here we shall be interested in more general mixtures and more general correlation functions. In particular, consider adding p spherical solute particles of radii $b_1,..., b_p$, respectively, centered at positions $\mathbf{x}_1,..., \mathbf{x}_p$, respectively, to a system of N equisized spherical solvent particles of radius R, centered at positions $\mathbf{r}_1,..., \mathbf{r}_N$, respectively, where N is sufficiently large to justify a statistical treatment. It is important to emphasize that the solvent particles of radius R represent the actual inclusions in the composite. The p solute particles are capable of excluding the centers of the solvent particles from spheres of radii $a_1,..., a_p$, respectively, surrounding the solute particles. Therefore, for $b_i > 0$, $a_i = R + b_i$. For $b_i = 0$ we shall allow the solute particles to penetrate the solvent particles, so that $a_i = R - c_i$ $(0 \leqslant c_i \leqslant R)$, where a_i is the minimum separation distance between solute and solvent

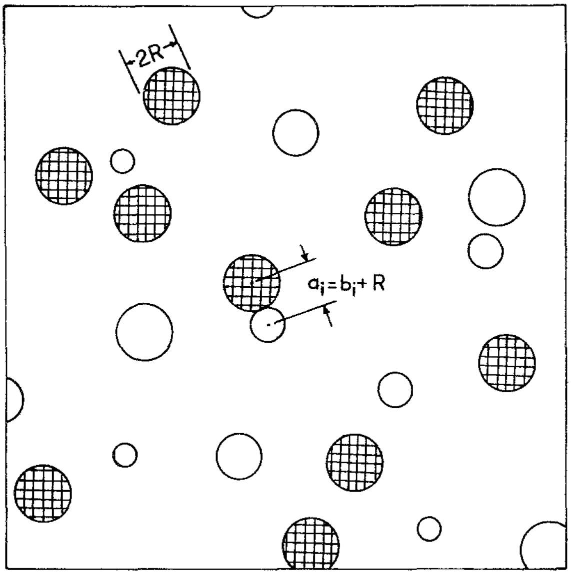

Fig. 1. Schematic description of the solute–solvent mixture for solute particles having arbitrary, nonzero radii. The solvent particles of radius R (which represent the actual inclusions in the composite) and solute particles with radii $b_i > 0$ are indicated by the shaded and by the unshaded particles, respectively.

centers. Figure 1 schematically describes this solute–solvent mixture for $b_i > 0$. For simplicity, we let the solute particles be perfectly penetrable to one another, i.e., they are spatially uncorrelated with respect to each other. Note that the solute particles merely serve to probe the space D_i and surface $\mathscr{S}_i$ available to them. In the simplest case of addition of a single solute particle of zero radius to the system of N inclusions, the space and surface (per unit volume) available to the solute particle are simply the matrix (or void) volume fraction ϕ $(=1-\phi_p$, where ϕ_p is the particle phase volume fraction) and specific surface s, respectively.

For the mixture described above it is desired to define a certain distribution function $G_n(\mathbf{x}^p; \mathbf{r}^q)$ in terms of certain characteristic functions described below. $G_n(\mathbf{x}^p; \mathbf{r}^q)$ is the n-point distribution function that characterizes the correlation associated with finding p solute particles with configuration $\mathbf{x}^p$ and q solvent particles with configuration $\mathbf{r}^q$, where $n = p + q$. Such quantities are generalizations of the solute–solvent radial distribution function used in the scaled-particle theory of Reiss *et al.*(22) If all the solute particles, for the case $q = 0$, have zero radius (i.e., $b_i = 0$ for all i) and $a_i = R$ for all i, then the G_n defined above reduces to the n-point matrix probability function, where $n = p$, i.e., $G_n(\mathbf{x}^n; \varnothing) = S_n(\mathbf{x}_n)$, where $\varnothing$

denotes the null set. If $p=1$ and the radius of the solute particle is taken to be zero such that $a_1=R$, then $G_n(\mathbf{x}_1;\mathbf{r}^q)$ is equal to the point/q-particle distribution function $G_q^{(1)}(\mathbf{x}_1;\mathbf{r}^q)$ defined in Ref. 16. We shall also be interested in defining and studying a still more general n-point distribution H_n (defined below), which not only characterizes the configuration of solute particles and a subset of the solvent particles, but describes the distribution of points on certain surfaces in the system. It is because of our interest in this latter quantity that requires us, as we shall see, to consider solute particles with nonzero radii.

The solvent particles are spatially distributed according to the N-particle probability density $P_N(\mathbf{r}^N)$, which characterizes the probability of finding the solvent particles $1, 2,..., N$ with configuration $\mathbf{r}^N$, respectively. P_N is assumed normalized to unity. Note that P_N is perfectly general, i.e., P_N may describe an equilibrium ensemble, as well as a nonequilibrium ensemble. The n-particle probability density described above is related to P_N through the following relation:

$$\rho_n(\mathbf{r}^n)=\frac{N!}{(N-n)!}\int P_N(\mathbf{r}^N)\,d\mathbf{r}^{N-n} \tag{2.1}$$

where $d\mathbf{r}^{N-n}\equiv d\mathbf{r}_{n+1}\cdots d\mathbf{r}_N$. The ensemble average of any many-body function $F(\mathbf{r}^N)$ is simply given by

$$\langle F(\mathbf{r}^N)\rangle=\int F(\mathbf{r}^N)\,P_N(\mathbf{r}^N)\,d\mathbf{r}^N \tag{2.2}$$

It is important to note that the solvent particles are, in general, distributed with arbitrary degree of impenetrability. The degree of impenetrability is characterized by some parameter λ whose value varies between zero (in the case of randomly centered spheres and thus completely uncorrelated, i.e., "fully penetrable spheres") and unity (in the instance of totally impenetrable spheres). Examples of sphere distributions involving intermediate values of λ include the permeable-sphere (PS) model(23) and the penetrable-concentric-shell (PCS) model.(24) In the PS model, spherical inclusions of radius R are assumed to be noninteracting when nonintersecting (i.e., when $r>2R$, where r is the distance between sphere centers), with probability of intersecting given by a radial distribution function $g(r)$ that is $1-\lambda$, independent of r, when $r<2R$. In the PCS model (depicted in Fig. 2) spheres of radius R are statistically distributed throughout space subject only to the condition of a mutually impenetrable core of radius λR, $0\leqslant\lambda\leqslant 1$. Each sphere of radius R may be thought of as being composed of an impenetrable core of radius λR, encompassed by a perfectly penetrable concentric shell of thickness

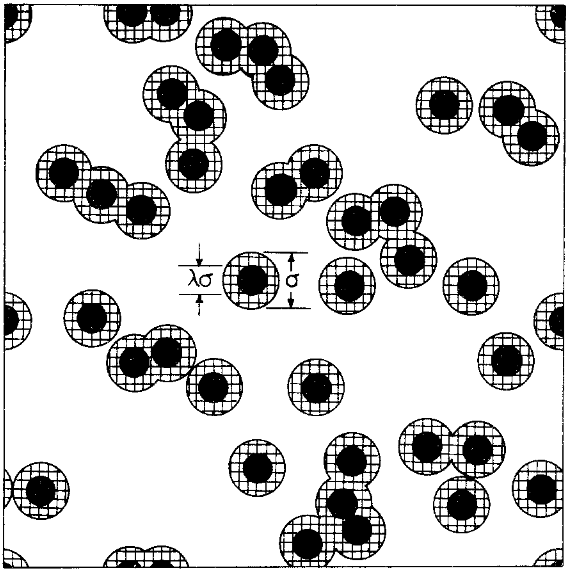

Fig. 2. A computer-generated realization of a distribution of disks of radius $R = \sigma/2$ (shaded region) in a matrix (unshaded region) in the PCS model.[24] The disks have an impenetrable core of diameter $\lambda\sigma$ indicated by the smaller, black circular regions. Here $\lambda = 0.5$ and the particle volume fraction $\phi_p = 1 - \phi = 0.3$.

$(1-\lambda)R$. Interpenetrable-sphere models enable one to study the effect of the degree of connectivity of the particle phase on the transport properties. The degree of connectivity of the individual phases may greatly influence the transport properties of two-phase media, particularly when the phase property values differ significantly. The PS and PCS models may serve as useful models of consolidated media, such as sandstones and other rocks, and sintered materials.

It is desired to define the G_n and H_n in terms of characteristic functions for the general case of a mixture of p solute particles of radii $b_1,..., b_p$, respectively, and N solvent particles of radius R. Since the ith solute particle is capable of excluding the centers of the solvent particles from spheres of radius a_i (where for $b_i > 0$, $a_i = R + b_i$ and for $b_i = 0$, $a_i = R - c_i$), then it is natural to associate with each solute particle i a subdivision of space into two regions: the space available to the ith solute particle (i.e., the space outside N spheres of radius a_i centered at $\mathbf{r}^N$) D_i, and the complement space D_i^*). The entire system is a domain of space $D(= D_i + D_i^*)$ of volume V. We define the characteristic function

$$I(\mathbf{x}; a_i) = \begin{cases} 1, & \mathbf{x} \in D_i \\ 0, & \text{otherwise} \end{cases} \tag{2.3}$$

This characteristic function can be related to the positions of the solvent particles in the following manner:

$$I(\mathbf{x}; a_i) = \prod_{j=1}^{N} [1 - m(y_j; a_i)] \tag{2.4a}$$

$$= 1 - \sum_{j=1}^{N} m(y_j; a_i) + \sum_{j<k}^{N} m(y_j; a_i)\, m(y_k; a_i) - \sum_{j<k<l}^{N} m(y_j; a_i)\, m(y_k; a_i)\, m(y_l; a_i) + \cdots \tag{2.4b}$$

where

$$m(y_j; a_i) = \begin{cases} 1, & y_j < a_i \\ 0, & \text{otherwise} \end{cases} \tag{2.5}$$

and $y_j = |\mathbf{x} - \mathbf{r}_j|$. The nth sum in Eq. (2.4b) is over all distinguishable n-tuplets of "interaction" spheres (i.e., spheres of radius a_i centered at $\mathbf{r}^N$) and thus contains $N!/(N-n)!\, n!$ terms. It arises because n-tuplets of interaction spheres may happen to simultaneously overlap.

Let $\mathcal{S}_i$ denote the surface between D_i and D_i^*. Then the characteristic function of $\mathcal{S}_i$, $M(\mathbf{r}; a_i)$, may be obtained from Eq. (2.4) by differentiating $-I$ with respect to a_i:

$$M(\mathbf{x}; a_i) = -\frac{\partial I(\mathbf{x}; a_i)}{\partial a_i} \tag{2.6a}$$

$$= \sum_{j=1}^{N} \delta(a_i - y_j) - \sum_{j<k}^{N} \delta(a_i - y_j)\, m(y_k; a_i) - \sum_{j<k}^{N} \delta(a_i - y_k)\, m(y_j; a_i) + \cdots \tag{2.6b}$$

where δ is the Dirac delta function. Clearly, $M(\mathbf{x}; a_i)$ is a function that is zero everywhere except when $\mathbf{x}$ describes a position on $\mathcal{S}_i$. Equations (2.4) and (2.6) generalize corresponding relations derived by Torquato and Stell$^{(11)}$ and by Torquato and Stell$^{(25)}$ and Chiew and Glandt,$^{(26)}$ respectively, for the special case in which all $b_i = 0$ and all $a_i = R$. The ensemble averages [cf. Eq. (2.2)] of I and M are simply the volume fraction $\phi_i(a_i)$ and specific surface $s_i(a_i)$ associated with the space D_i and the surface $\mathcal{S}_i$, respectively. It is only when all $b_i = 0$ and all $a_i = R$ that $\langle I \rangle$ and $\langle M \rangle$ are, respectively, equal to the volume fraction of matrix ϕ and the specific surface of the particle–matrix interface s.

More generally, we have

$$G_n(\mathbf{x}^n; \varnothing) = \left\langle \prod_{i=1}^{n} I(\mathbf{x}_i; a_i) \right\rangle \tag{2.7a}$$

= Correlation associated with finding a point at $\mathbf{x}_1$ in D_1, a point at $\mathbf{x}_2$ in D_2, etc. (2.7b)

= Correlation associated with finding solute particles $1,..., n$ of radii $b_1,..., b_n$, respectively, with configuration $\mathbf{x}^n$, respectively (2.7c)

= Probability that n spheres of radii $a_1,..., a_n$, respectively, are empty of the centers of solvent particles (2.7d)

We are actually interested in defining the still more general n-point distribution function $G_n(\mathbf{x}^p; \mathbf{r}^q)$ in which a subset of the n points refer to solute particles and the remaining points refer to solvent particles. Given (2.7), it follows that

$$G_n(\mathbf{x}^p; \mathbf{r}^q) = \frac{N!}{(N-q)!} \int \prod_{i=1}^{p} I(\mathbf{x}_i; a_i)\, P_N(\mathbf{r}^N)\, d\mathbf{r}^{N-q} \tag{2.8a}$$

= Correlation associated with finding a solute particle of radius b_1 centered at $\mathbf{x}_1,...,$ and another solute particle of radius b_p centered at $\mathbf{x}_p$, and of finding q solvent particles with configuration $\mathbf{r}^q$, where $n = p + q$ (2.8b)

The dependence on $\mathbf{r}^q$ arises because the integrations are over all solvent particles not included in the subset of the q solvent particles. The factor $N!/(N-q)!$ in Eq. (2.8) accounts for the indistinguishability of the solvent particles. Note that for the case $q = 0$, Eq. (2.8) reduces to Eq. (2.7). Moreover, in the instance $p = 0$, G_n is identical to the n-particle probability density ρ_n [i.e., Eq. (2.8) reduces to Eq. (2.1)].

Employing Eqs. (2.6a) and (2.8), it is clear that

$$H_n(\mathbf{x}^m; \mathbf{x}^{p-m}; \mathbf{r}^q) = (-1)^m \frac{\partial}{\partial a_1} \cdots \frac{\partial}{\partial a_m} G_n(\mathbf{x}^p; \mathbf{r}^q) \tag{2.9a}$$

$$= \frac{N!}{(N-q)!} \int \left[\prod_{i=1}^{m} M(\mathbf{x}_i; a_i) \right] \left[\prod_{i=m+1}^{p} I(\mathbf{x}_i; a_i) \right] \times P_N(\mathbf{r}^N)\, d\mathbf{r}^{N-q} \tag{2.9b}$$

$=$ Correlation associated with finding the center of a solute particle of radius b_1 at $\mathbf{x}_1$ on $\mathscr{S}_1,\ldots,$ and the center of a solute particle of radius b_m at $\mathbf{x}_m$ on $\mathscr{S}_m$, and the center of a solute particle of radius b_{m+1} and $\mathbf{x}_{m+1}$ in $D_{m+1},\ldots,$ and the center of a solute particle of radius b_p at $\mathbf{x}_p$ in D_p, and of finding any q solvent particles with configuration $\mathbf{r}^q$, where $\mathbf{x}^{p-m} \equiv \{\mathbf{x}_{m+1},\ldots, \mathbf{x}_p\}$ and $n = p + q$ (2.9c)

The n-point distribution function H_n is new and is the most general statistical quantity that we shall deal with in this paper. From this single function one can obtain all of the correlation functions described in the introduction (by setting $b_i = 0$ and $a_i = R$, $i = 1,\ldots, p$), i.e., the n-point matrix probability functions,(11) the surface–surface and surface–matrix correlation functions(17) and their generalizations, the surface–particle correlation function[2] and its generalizations, and the point/n-particle distribution functions.(16,18) This is the first time this connection has been noted. Note that in the case of a statistically homogeneous system, $P_N(\mathbf{r}^N)$ is invariant under translation and thus implies that the G_n and H_n will be functions of relative positions.

2.2. Some Properties of the *n*-Point Functions

In studying the asymptotic properties of G_n and H_n, it will suffice to focus our attention on H_n alone, since G_n is a special case of H_n, i.e., $H_n(\mathbf{x}^m; \mathbf{x}^{p-m}; \mathbf{r}^q) = G_n(\mathbf{x}^p; \mathbf{r}^q)$ when $m = 0$.

Since H_n is a joint distribution function, one has the normalization condition

$$\int H_n(\mathbf{x}^m; \mathbf{x}^{p-m}; \mathbf{r}^q)\, d\mathbf{r}^q = \frac{N!}{(N-q)!} H_p(\mathbf{x}^m; \mathbf{x}^{p-m}; \varnothing) \tag{2.10}$$

where $q = n - p$. This is arrived at by integrating Eq. (2.9b) over the positions $\mathbf{r}^q$.

---

[2] Weissberg and Prager(18) actually define the quantity $R^{(1)}(\mathbf{y}_1; \hat{\mathbf{y}}_2)$, which gives the conditional probability that if $\mathbf{x}_1$ is on the surface of a sphere centered at $\mathbf{r}_2$ and $\hat{\mathbf{y}}_2 = \mathbf{y}_2/|\mathbf{y}_2|$, then there will be a sphere centered at $\mathbf{r}_1$. It is easily shown that

$$\frac{s}{4\pi} \int R^{(1)}(\mathbf{y}_1; \hat{\mathbf{y}}_2)\, d\hat{\mathbf{y}}_2 = -e(y_1; R) \frac{\partial}{\partial a_1} \left[\frac{G_2(\mathbf{x}_1; \mathbf{r}_1)}{e(y_1; a_1)} \right]_{a_1 = R} = \bar{F}_{\rm sp}(y_1)$$

where $d\hat{\mathbf{y}}_2$ denotes an element of solid angle on sphere 2, s is the specific surface, $\bar{F}_{\rm sp}(y_1)$ is the contribution to $F_{\rm sp}$ (or H_2) when $\mathbf{x}_1$ is on the surface of a sphere and $\mathbf{r}_1$ describes the center of another sphere, and $e(y_1; R)$ is defined by (3.1b).

We now examine the asymptotic behavior of the H_n. The set $(\mathbf{x}^m; \mathbf{x}^{p-m}; \mathbf{r}^q)$ is partitioned into $L = L(\alpha)$ disjoint subsets, where $\{\alpha\} = \{\alpha_1; \alpha_2; ...; \alpha_L\}$ is any partition of the aforementioned set, $\{\alpha_i\}$ is the ith subset, and n_i is the number of elements in $\{\alpha_i\}$. The subset $\{\alpha_i\}$ is in turn partitioned into three subsets, i.e., $\{\alpha_i^{(1)}; \alpha_i^{(2)}; \alpha_i^{(3)}\}$, where $\{\alpha_i^{(1)}\}$ contains elements of the subset $\mathbf{x}^m$, $\{\alpha_i^{(2)}\}$ contains elements of the subset $\mathbf{x}^{p-m}$, and $\{\alpha_i^{(3)}\}$ contains elements of the subset $\mathbf{r}^q$. Let $n_i^{(j)}$, $j = 1, 2$, or 3, denote the number of elements in $\{\alpha_i^{(j)}\}$. Then $\sum_{i=1}^{L} n_i^{(1)} = m$, $\sum_{i=1}^{L} n_i^{(2)} = p - m$, and $\sum_{i=1}^{L} n_i^{(3)} = q$. Let all of the relative distances between the n_i elements of the subset $\{\alpha_i\}$ remain bounded, and let F_{α_i} be the polyhedron with n_i vertices located at the positions associated with the subset $\{\alpha_i\}$. We denote the centroid of the F_{α_i} by $\mathbf{R}_i$. Assuming no long-range order, we have that

$$\lim_{\text{all } R_{jk} \to \infty} H_n(\mathbf{x}^m; \mathbf{x}^{p-m}; \mathbf{r}^q) = \prod_{i=1}^{L} H_{n_i}(\alpha_i^{(1)}; \alpha_i^{(2)}; \alpha_i^{(3)}) \tag{2.11}$$

where $R_{jk} = |\mathbf{R}_k - \mathbf{R}_j|$ is the relative distance between the centroids of F_{α_j} and F_{α_k}, such that $1 \leqslant j < k \leqslant L$.

From Eq. (2.9b) it follows that when $r + 1$ of the elements (points) of $\mathbf{x}^m$ coincide and $t + 1$ of the elements (points) of $\mathbf{x}^{p-m}$ coincide, then

$$H_n(\mathbf{x}^m; \mathbf{x}^{p-m}; \mathbf{r}^q) \to H_{n-r-t}(\beta_1; \beta_2; \mathbf{r}^q) \tag{2.12}$$

where $\{\beta_1\}$ and $\{\beta_2\}$ denote the subsets associated with the elements of $\mathbf{x}^m$ and $\mathbf{x}^{p-m}$, respectively, that do not coincide.

In the PCS model,$^{(24)}$ $H_n(\mathbf{x}^m; \mathbf{x}^{p-m}; \mathbf{r}^q)$ is identically zero for certain $\mathbf{r}^q$. In particular, we have

$$H_n(\mathbf{x}^m; \mathbf{x}^{p-m}; \mathbf{r}^q) = 0 \qquad \text{if} \quad |\mathbf{r}_i - \mathbf{r}_j| < 2\lambda R \tag{2.13}$$

for any $i \neq j$ such that $1 \leqslant i \leqslant q$ and $1 \leqslant j \leqslant q$.

3. REPRESENTATIONS OF G_n AND H_n

It is desired to derive series representations of both G_n and H_n for the mixture described in Section 2. Once the series representation of the G_n is derived, we may obtain the corresponding expression for the H_n from definition (2.9a). We note that, in general, the solvent particles are distributed with arbitrary degree of penetrability. Furthermore, the results obtained here are not restricted to three-dimensional spherical particles and so they hold for rods in one dimension and circular disks in two dimensions. The formal results obtained here are also easily extended to dispersions of spheres (disks) with a size distribution and to distributions of equisized inclusions, whose configuration is completely specified by center-of-mass coordinates (e.g., oriented ellipsoids, cubes, squares, etc.), by appropriately generalizing the characteristic functions I, Eq. (2.3), and M, Eq. (2.6). This, however, is not done here. We now proceed to obtain two equivalent but topologically different representations of the G_n and the H_n.

3.1. Kirkwood–Salsburg Representation

The product of the characteristic functions $\prod_{i=1}^{p} I(\mathbf{x}_i; a_i)$ may be written as follows:

$$\begin{aligned}\prod_{i=1}^{p} I(\mathbf{x}_i; a_i) &= \left\{\prod_{k=1}^{q} e(y_{1k}; a_1)\right\}\left\{\prod_{k=q+1}^{N} [1-m(y_{1k}; a_1)]\right\}\prod_{i=2}^{p} I(\mathbf{x}_i; a_i)\\ &= \prod_{k=1}^{q} e(y_{1k}; a_1)\left[\prod_{i=2}^{p} I(\mathbf{x}_i; a_i) - \sum_{j=q+1}^{N} m(y_{1j}; a_1)\prod_{i=2}^{p} I(\mathbf{x}_i; a_i)\right.\\ &\quad \left. + \sum_{\substack{j=q+1\\ j<k}}^{N} m(y_{1j}; a_1)\, m(y_{1k}; a_1)\prod_{i=2}^{p} I(\mathbf{x}_i; a_i) - \cdots\right] \end{aligned}\tag{3.1a}$$

$$\text{where}\quad e(y_{ij}; a_i) = 1 - m(y_{ij}; a_i) = \begin{cases} 0, & y_{ij} < a_i\\ 1, & \text{otherwise}\end{cases}\tag{3.1b}$$

and $y_{ij} = |\mathbf{x}_i - \mathbf{r}_j|$. Here we have made use of Eq. (2.4b). Note that attention here is focused on solute particle 1 and on q of the solvent particles. Combination of Eqs. (2.8) and (3.1) gives

$$\begin{aligned}&\frac{G_n(\mathbf{x}^p; \mathbf{r}^q)}{\prod_{k=1}^{q} e(y_{1k}; a_1)}\\ &\quad = G_{n-1}(\mathbf{x}^{p-1}; \mathbf{r}^q) - \frac{N!}{(N-q-1)!}\int m(y_{1,q+1}; a_1)\\ &\qquad \times \prod_{i=2}^{p} I(\mathbf{x}_i; a_i)\, P_N(\mathbf{r}^N)\, d\mathbf{r}^{N-q}\\ &\qquad + \frac{N!}{(N-q-2)!\,2!}\int m(y_{1,q+1}; a_1)\, m(y_{1,q+2}; a_1)\\ &\qquad \times \prod_{i=2}^{p} I(\mathbf{x}_i; a_1)\, P_N(\mathbf{r}^N)\, d\mathbf{r}^{N-q} - \cdots \end{aligned}\tag{3.2}$$

In general, for a statistically homogeneous medium, we have

$$G_n(\mathbf{x}^p; \mathbf{r}^q) = \sum_{s=0}^{\infty} (-1)^s\, G_n^{\mathrm{KS}(s)}(\mathbf{x}^p; \mathbf{r}^q), \qquad n = p + q\tag{3.3}$$

where

$$G_n^{\mathrm{KS}(s)}(\mathbf{x}^p; \mathbf{r}^q) = \frac{\prod_{k=1}^{q} e(y_{1k}; a_1)}{s!} \int G_{n+s-1}(\mathbf{x}^{p-1}; \mathbf{r}^{q+s}) \prod_{j=q+1}^{q+s} m(y_{1j}; a_1)\, d\mathbf{r}_j \tag{3.4}$$

and

$$G_n^{\mathrm{KS}(0)}(\mathbf{x}^p; \mathbf{r}^q) \equiv G_{n-1}(\mathbf{x}^{p-1}; \mathbf{r}^q) \prod_{k=1}^{q} e(y_{1k}; a_1) \tag{3.5}$$

It is important to note that Eq. (3.3) applies to equilibrium as well as nonequilibrium ensembles. Interestingly, for an equilibrium distribution of q solute particles and N solvent particles, in the limit of infinite dilution of each solute species, Eq. (3.3) is isomorphic with the Kirkwood–Salsburg representation of the n-point distribution function associated with such a liquid mixture. For this reason we refer to Eq. (3.3) as the Kirkwood–Salsburg representation of the G_n. Hence, for an equilibrium distribution, Eq. (3.3) could have been derived using the general set of integral equations for a mixture derived by Baer and Lebowitz(27) (of which the Kirkwood–Salsburg series is a special case) if the following correspondence is made:

$$\lim_{\substack{\rho^{(i)} \to 0 \\ z^{(i)} \to 0 \\ \text{all } i}} \frac{\rho_n(\mathbf{x}^p; \mathbf{r}^q)}{\prod_{i=1}^{p} z^{(i)}} = G_n(\mathbf{x}^p; \mathbf{r}^q) \tag{3.6}$$

where $\rho^{(i)}$ and $z^{(i)}$ are the number densities and fugacities associated with the ith solute species $(i = 1,..., p)$, $\rho_n(\mathbf{x}^p; \mathbf{r}^q)$ is the n-particle probability density associated with finding the solute particles with configuration $\mathbf{x}^p$ and the solvent particles with configuration $\mathbf{r}^q$, and the limiting process specifies that $\rho^{(i)} \to 0$ and $z^{(i)} \to 0$, for $i = 1,..., p$. The left-hand side of Eq. (3.6) comes from the left-hand side of Eq. (3.9) of Ref. 27. For a statistically homogeneous medium (i.e., in the thermodynamic limit, $N \to \infty$, $V \to \infty$ such that $\rho = N/V$ remains bounded), Eq. (3.6) leads to

$$\rho^q \prod_{i=1}^{p} \phi_i(a_i)\, g_n(\mathbf{x}^p; \mathbf{r}^q) = G_n(\mathbf{x}^p; \mathbf{r}^q) \tag{3.7}$$

where

$$g_n(\mathbf{x}^p; \mathbf{r}^q) = \frac{\rho_n(\mathbf{x}^p; \mathbf{r}^q)}{\rho^q \prod_{i=1}^{p} \rho^{(i)}} \tag{3.8}$$

and

$$\phi_i(a_i) = \lim_{\substack{\rho^{(i)} \to 0 \\ z^{(i)} \to 0}} \frac{\rho^{(i)}}{z^{(i)}} \tag{3.9}$$

and ρ is the number density of the solvent particles. Note that when $b_i = 0$ and $a_i = R$, $\phi_i(R)$ is simply the fraction of the space available to the ith solute particle, i.e., the matrix volume fraction ϕ.

The connection between statistical mechanical hierarchies and n-point distribution functions that arise in composite-media problems was first recognized by Torquato and Stell,[(12)] who showed that the Mayer–Montroll and Kirkwood–Salsburg equations for n point solute particles and N solvent particles become equations for the n-point matrix probability functions S_n. When $q = 0$, $b_i = 0$, and $a_i = R$ ($i = 1,..., n$), Eq. (3.3) reduces to the Kirkwood–Salsburg representation of the S_n derived in Ref. 12.

Combining Eqs. (2.9) and (3.3) gives a series representation of the new and more general function H_n:

$$H_n(\mathbf{x}^m; \mathbf{x}^{p-m}; \mathbf{r}^q) = \sum_{s=0}^{\infty} (-1)^s H_n^{\mathrm{KS}(s)}(\mathbf{x}^m; \mathbf{x}^{p-m}; \mathbf{r}^q), \qquad n = p + q \tag{3.10}$$

where

$$H_n^{\mathrm{KS}(s)}(\mathbf{x}^m; \mathbf{x}^{p-m}; \mathbf{r}^q) = (-1)^m \frac{\partial}{\partial a_1} \cdots \frac{\partial}{\partial a_m} G_n^{\mathrm{KS}(s)}(\mathbf{x}^p; \mathbf{r}^q) \tag{3.11}$$

The $G_n^{\mathrm{KS}(s)}$ are given by Eq. (3.4). Although (3.10) for the H_n is more general than (3.3) for the G_n, we refer to it as the Kirkwood–Salsburg representation of the H_n because it is obtained from Definition (2.9a) and Series (3.3).

3.2. Mayer Representation

The product of the characteristic functions $\prod_{i=1}^{p} I(\mathbf{x}_i; a_i)$ may also be rewritten in the following manner:

$$\begin{aligned}\prod_{i=1}^{p} I(\mathbf{x}_i; a_i) &= \left\{\prod_{l=1}^{q} \prod_{k=1}^{p} e(y_{kl}; a_k)\right\} \prod_{l=q+1}^{N} \prod_{k=1}^{p} [1 - m(y_{kl}; a_k)] \\ &= \prod_{l=1}^{q} \prod_{k=1}^{p} e(y_{kl}; a_k) \Bigg[1 - \sum_{i=q+1}^{N} m^{(p)}(\mathbf{x}^p; \mathbf{r}_i) \\ &\quad + \sum_{\substack{i=q+1 \\ i<j}}^{N} m^{(p)}(\mathbf{x}^p; \mathbf{r}_i)\, m^{(p)}(\mathbf{x}^p; \mathbf{r}_j) - \cdots \Bigg]\end{aligned} \tag{3.12}$$

where

$$m^{(p)}(\mathbf{x}^p; \mathbf{r}_j) = 1 - \prod_{i=1}^{p} [1 - m(y_{ij}; a_i)] \tag{3.13}$$

In arriving at Eq. (3.12), we have employed Eq. (2.4b). Unlike the previous case, however, attention here is focused on all p solute particles and q solvent particles. Equations (2.8) and (3.12) lead to

$$\frac{G_n(\mathbf{x}^p; \mathbf{r}^q)}{\prod_{l=1}^{q} \prod_{k=1}^{p} e(y_{kl}; a_k)} = \rho_q(\mathbf{r}^q) - \int m^{(p)}(\mathbf{x}^p; \mathbf{r}_{q+1})\, \rho_{q+1}(\mathbf{r}^{q+1})\, d\mathbf{r}_{q+1} + \frac{1}{2!} \int m^{(p)}(\mathbf{x}^p; \mathbf{r}_{q+1})\, m^{(p)}(\mathbf{x}^p; \mathbf{r}_{q+2})\, \rho_{q+2}(\mathbf{r}^{q+2})\, d\mathbf{r}_{q+1}\, d\mathbf{r}_{q+2} - \cdots \tag{3.14}$$

In general, for a statistically homogeneous medium,

$$G_n(\mathbf{x}^p; \mathbf{r}^q) = \sum_{s=0}^{\infty} (-1)^s\, G_n^{\mathrm{M}(s)}(\mathbf{x}^p; \mathbf{r}^q), \qquad n = p + q \tag{3.15}$$

where

$$G_n^{\mathrm{M}(s)}(\mathbf{x}^p; \mathbf{r}^q) = \frac{\prod_{l=1}^{q} \prod_{k=1}^{p} e(y_{kl}; a_k)}{s!} \times \int \rho_{q+s}(\mathbf{r}^{q+s}) \prod_{j=q+1}^{q+s} m^{(p)}(\mathbf{x}^p; \mathbf{r}_j)\, d\mathbf{r}_j \tag{3.16}$$

and

$$G_n^{\mathrm{M}(0)}(\mathbf{x}^p; \mathbf{r}^q) \equiv \rho_q(\mathbf{r}^q) \prod_{l=1}^{q} \prod_{k=1}^{p} e(y_{kl}; a_k) \tag{3.17}$$

Equation (3.15) is a different and new representation of the G_n. As in the previous case, it applies to general ensembles. In the context of liquid-state theory, an expression of this type was derived by Mayer(28) for a single-component fluid in thermal equilibrium. Accordingly, we refer to Eq. (3.15) as the Mayer representation of the G_n. This is the first time the Mayer representation has been used in the context of composite media problems. Note that unlike the sth term of Eq. (3.3), which involves integrands containing the G_{n+s-1}, the corresponding term in Eq. (3.15) involves integrands containing the $(q+s)$-particle probability density $\rho_{q+s}(\mathbf{r}^{q+s})$ associated with the solvent particles only. Since the ρ_n are in principle given information, the Mayer representation (3.15) will prove to be superior to the Kirkwood–Salsburg representation for the purposes of exactly evaluating the G_n. However, the latter representation provides a means of bounding the G_n that is more powerful than the former (see Section 3.3).

For an equilibrium distribution, Eq. (3.15) could have been derived employing the general results of Baer and Lebowitz$^{(27)}$ and Eq. (3.6). Note that when $q=0$, $b_i=0$, and $a_i=R$ $(i=1,..., p)$, the Mayer representation of the G_n become the Mayer–Montroll equations for the S_n derived by Torquato and Stell.$^{(12)}$ Moreover, when $p=1$, $b_i=0$, and $a_i=R$ $(i=1,..., p)$, Eq. (3.15) reduces to the Kirkwood–Salsburg equations for the point/n-particle distribution functions[3] obtained by Torquato.$^{(16)}$

Combination of Eqs. (2.9a) and (3.15) yields what we refer to as the Mayer representation of the H_n:

$$H_n(\mathbf{x}^m; \mathbf{x}^{p-m}; \mathbf{r}^q) = \sum_{s=0}^{\infty} (-1)^s H_n^{\mathrm{M}(s)}(\mathbf{x}^m; \mathbf{x}^{p-m}; \mathbf{r}^q), \qquad n=p+q \tag{3.18}$$

where

$$H_n^{\mathrm{M}(s)}(\mathbf{x}^m; \mathbf{x}^{p-m}; \mathbf{r}^q) = (-1)^m \frac{\partial}{\partial a_1} \cdots \frac{\partial}{\partial a_m} G_n^{\mathrm{M}(s)}(\mathbf{x}^p; \mathbf{r}^q) \tag{3.19}$$

The $G_n^{\mathrm{M}(s)}$ are given by Eq. (3.16). Note that (3.18) is new and more general than (3.15).

3.3. Bounding Properties

It is well known that hierarchies of the type given by (3.3) and (3.15) allow one to rigorously bound the distribution function.$^{(12,27)}$ This property was exploited by Torquato and Stell$^{(12)}$ to yield bounds on the S_n. In particular, here we have

$$G_n \left\} \begin{matrix} \geqslant \\ \leqslant \end{matrix} \right\{ Q_n^{\mathrm{KS}(l)} \qquad \begin{matrix} \text{for } l \text{ odd} \\ \text{for } l \text{ even} \end{matrix} \tag{3.20}$$

and

$$G_n \left\} \begin{matrix} \geqslant \\ \leqslant \end{matrix} \right\{ Q_n^{\mathrm{M}(l)} \qquad \begin{matrix} \text{for } l \text{ odd} \\ \text{for } l \text{ even} \end{matrix} \tag{3.21}$$

where the $Q_n^{(l)}$ are the partial sums

$$Q_n^{\mathrm{KS}(l)} = \sum_{s=0}^{l} (-1)^s G_n^{\mathrm{KS}(s)} \tag{3.22}$$

---

[3] Note that in this instance comparison of Eq. (3.15) for $G_2(\mathbf{x}_1; \mathbf{r}_1)$ at $y_{11} = |\mathbf{x}_1 - \mathbf{r}_1| = R$ and of Eq. (3.18) for $H_1(\mathbf{x}_1) = s\,(a_1 = R) = s$, for an isotropic system, yields $s = 4\pi R^2 G_2(y_{11} = R)$. Since $G_2(y_{11} = R)/\rho$ takes on its maximum value of unity for the case of totally impenetrable spheres and its minimum value of $\phi = \exp(-\rho 4\pi R^3/3)$ for the case of fully penetrable spheres, it may be regarded as the fraction of exposed interface area.

and

$$Q_n^{\mathrm{M}(l)} = \sum_{s=0}^{l} (-1)^s G_n^{\mathrm{M}(s)} \tag{3.23}$$

Here $G_n^{\mathrm{KS}(s)}$ and $G_n^{\mathrm{M}(s)}$ are given by Eqs. (3.4) and (3.16), respectively.

Similarly, from Eqs. (3.10), (3.11), and (3.18)–(3.21), we find for even m

$$\left.H_n\right\} \begin{matrix} \geqslant \\ \leqslant \end{matrix} \left\{W_n^{\mathrm{KS}(l)}\right. \qquad \begin{matrix} \text{for } l \text{ odd} \\ \text{for } l \text{ even} \end{matrix} \tag{3.24}$$

and

$$\left.H_n\right\} \begin{matrix} \geqslant \\ \leqslant \end{matrix} \left\{W_n^{\mathrm{M}(l)}\right. \qquad \begin{matrix} \text{for } l \text{ odd} \\ \text{for } l \text{ even} \end{matrix} \tag{3.25}$$

and for odd m

$$\left.H_n\right\} \begin{matrix} \geqslant \\ \leqslant \end{matrix} \left\{W_n^{\mathrm{KS}(l)}\right. \qquad \begin{matrix} \text{for } l \text{ even} \\ \text{for } l \text{ odd} \end{matrix} \tag{3.26}$$

and

$$\left.H_n\right\} \begin{matrix} \geqslant \\ \leqslant \end{matrix} \left\{W_n^{\mathrm{M}(l)}\right. \qquad \begin{matrix} \text{for } l \text{ even} \\ \text{for } l \text{ odd} \end{matrix} \tag{3.27}$$

where the $W_n^{(l)}$ are the partial sums

$$W_n^{\mathrm{KS}(l)} = \sum_{s=0}^{l} (-1)^s H_n^{\mathrm{KS}(s)} \tag{3.28}$$

and

$$W_n^{\mathrm{M}(l)} = \sum_{s=0}^{l} (-1)^s H_n^{\mathrm{M}(s)} \tag{3.29}$$

The $H_n^{\mathrm{KS}(s)}$ and $H_n^{\mathrm{M}(s)}$ are, respectively, given by Eqs. (3.11) and (3.19).

The fact that we have a succession of upper and lower bounds on G_n and H_n does not necessarily imply that $G_n^{(s)}$ and $H_n^{(s)}$ uniformly decreases in absolute value as s increases, i.e., that the bounds are successively better and better. However, there will be instances in which the series for G_n and H_n will be truncated (i.e., for certain distributions of solvent particles there exists some $s > k > 0$ such that $G_n^{(s)} = H_n^{(s)} = 0$ for all $s > k$).

For example, consider the series for the G_n for a system consisting of p point solute particles (where $a_i = R$ for all i) and N totally impenetrable spherical solvent particles of radius R. For such a medium, the terms of the Kirkwood–Salsburg infinite series (3.3) are identically zero for all $s > 1$, i.e.,

$$G_n(\mathbf{x}^p; \mathbf{r}^q) = G_{n-1}(\mathbf{x}^{p-1}; \mathbf{r}^q) - \int G_n(\mathbf{x}^{p-1}; \mathbf{r}^{q+1})\, m(y_{1,q+1}; R)\, d\mathbf{r}_1 \tag{3.30}$$

This follows since the product

$$m(y_{1,q+1}; R)\, m(y_{1,q+2}; R)\, G_{n+s-1}(\mathbf{x}^{p-1}; \mathbf{r}^{q+s})$$

appearing in the sth term in (3.3) is identically zero for all $s > 1$, since $m(y; R) = 0$ for $y > R$ and $G_n(\mathbf{x}^p; \mathbf{r}^q) = 0$ for all $|\mathbf{r}_i - \mathbf{r}_j| < 2R$, for any i and j such that $1 \leqslant i < j \leqslant n$. Similarly, the terms of the Mayer series (3.15) are identically zero for all $s > p$ since the product

$$\rho_{q+s}(\mathbf{r}^{q+s}) \prod_{j=q+1}^{q+s} m^{(p)}(\mathbf{x}^p; \mathbf{r}_j)$$

appearing in the sth term in (3.15) is identically zero for all $s > p$, i.e.,

$$G_n(\mathbf{x}^p; \mathbf{r}^q) = \sum_{s=0}^{p} (-1)^s\, G_n^{\mathrm{M}(s)}(\mathbf{x}^p; \mathbf{r}^q) \tag{3.31}$$

For such a system, the corresponding series for the H_n truncates after the same number of terms.

The Kirkwood–Salsburg representation provides a means of bounding the distribution functions that is more powerful than the Mayer representation. To illustrate this point, we examine the bounds on G_2 and G_3 for a mixture of point solute particles (where $a_i = R$ for all i) and N totally impenetrable solvent particles. When $n = 2$ the Kirkwood–Salsburg and Mayer representations are identical and hence application of either (3.20) and (3.21) yields

$$G_2(\mathbf{x}_1; \mathbf{r}_1) \leqslant \rho_1(\mathbf{r}_1) \tag{3.32}$$

and

$$G_2(\mathbf{x}_1 : \mathbf{r}_1) = \rho_1(\mathbf{r}_1) - \int \rho_2(\mathbf{r}_1, \mathbf{r}_2)\, m(y_{12}; R)\, d\mathbf{r}_2 \tag{3.33}$$

For homogeneous systems, $\rho_1(\mathbf{r}_1)$ is simply the number density ρ. For $n = 3$, the two series representations are not topologically identical. The Kirkwood–Salsburg inequality of (3.20) gives

$$G_3(\mathbf{x}_1, \mathbf{x}_2; \mathbf{r}_1) \leqslant G_2(\mathbf{x}_2; \mathbf{r}_1) \tag{3.34}$$

and

$$G_3(\mathbf{x}_1, \mathbf{x}_2; \mathbf{r}_1) = G_2(\mathbf{x}_2; \mathbf{r}_1) - \int G_3(\mathbf{x}_2; \mathbf{r}_1, \mathbf{r}_2)\, m(y_{12}; R)\, d\mathbf{r}_2 \tag{3.35}$$

On the other hand, the Mayer inequality (3.21) yields

$$G_3(\mathbf{x}_1, \mathbf{x}_2; \mathbf{r}_1) \leqslant \rho_1(\mathbf{r}_1) \tag{3.36}$$

$$G_3(\mathbf{x}_1, \mathbf{x}_2; \mathbf{r}_1) \geqslant \rho_1(\mathbf{r}_1) - \int \rho_2(\mathbf{r}_1, \mathbf{r}_2)\, m^{(2)}(\mathbf{x}_1, \mathbf{x}_2; \mathbf{r}_2)\, d\mathbf{r}_2 \tag{3.37}$$

$$\begin{aligned} G_3(\mathbf{x}_1, \mathbf{x}_2; \mathbf{r}_1) = {} & \rho_1(\mathbf{r}_1) - \int \rho_2(\mathbf{r}_1, \mathbf{r}_2)\, m^{(2)}(\mathbf{x}_1, \mathbf{x}_2; \mathbf{r}_2)\, d\mathbf{r}_2 \\ & + \frac{1}{2} \int \rho_3(\mathbf{r}_1, \mathbf{r}_2, \mathbf{r}_3)\, m^{(2)}(\mathbf{x}_1, \mathbf{x}_2; \mathbf{r}_2) \\ & \times m^{(2)}(\mathbf{x}_1, \mathbf{x}_2; \mathbf{r}_3)\, d\mathbf{r}_2\, d\mathbf{r}_3 \end{aligned} \tag{3.38}$$

Employing inequality (3.32), it is clear that (3.34) provides a better upper bound on G_3 than does (3.36). When $\mathbf{x}_1$ coincides with $\mathbf{x}_2$, (3.34), unlike (3.36), is exact. When $\mathbf{x}_1$, $\mathbf{x}_2$, and $\mathbf{r}_1$ are far apart from one another in a homogeneous system, $G_2 \to \phi\rho$ and $G_3 \to \phi^2\rho$ [cf. Eq. (2.11)], and hence, although the upper bound (3.34) is not exact in this case, it is sharper than (3.36). Relation (3.35), which is exact, obviously provides a better lower bound on G_3 than does inequality (3.37). In general, for any n, the Kirkwood–Salsburg, rather than the Mayer, representation will provide sharper bounds on the distribution function.

4. APPLICATIONS

In the previous section we derived two different series representations of the general n-point distribution function H_n. We now have a means of systematically calculating the H_n and, hence, bounds on effective properties that depend upon H_n, for dispersions of spheres distributed with arbitrary degree of impenetrability λ. In many applications we shall be interested in H_n in the limit that the radii of the solute particles become zero such that $a_i = R$, for all i. For example, in this limit, the n-point matrix probability function$^{(11)}$ and the point/q-particle function$^{(16,18)}$ (which actually is an n-point distribution function, $n = 1 + q$) are given respectively by

$$S_n(\mathbf{x}^n) = H_n(\varnothing, \mathbf{x}^n; \varnothing) = G_n(\mathbf{x}^n; \varnothing) \tag{4.1}$$

and

$$G_q^{(1)}(\mathbf{x}_1; \mathbf{r}^q) = H_n(\varnothing; \mathbf{x}_1; r^q) = G_n(\mathbf{x}_1; \mathbf{r}^q), \qquad n = 1 + q \tag{4.2}$$

Similarly, in this limit, the two-point surface correlation functions[17,18] are given by

$$F_{\mathrm{sm}}(\mathbf{x}_1, \mathbf{x}_2) = H_2(\mathbf{x}_1; \mathbf{x}_2; \varnothing) \tag{4.3}$$

$$F_{\mathrm{ss}}(\mathbf{x}_1, \mathbf{x}_2) = H_2(\mathbf{x}_1, \mathbf{x}_2; \varnothing; \varnothing) \tag{4.4}$$

$$F_{\mathrm{sp}}(\mathbf{x}_1, \mathbf{r}_1) = H_2(\mathbf{x}_1; \varnothing; \mathbf{r}_1) \tag{4.5}$$

Three-point surface correlation functions (e.g., F_{ssm}, F_{ssp}, F_{smp}, etc.) and their n-point generalizations can be obtained from the H_n in a similar fashion.

In some cases, the sizes of the solute or "test" particles that one wishes to introduce in a porous medium are not always negligible compared to the pore size and hence the distribution functions will depend upon the relative size of the particle and pore.[29] Our general series representations of the H_n (derived in the previous section) are clearly capable of characterizing the microstructure in such instances, since the b_i are, in general, nonzero. Such generalized quantities have a particularly simple application in the theory of gel chromatography.[30]

In this section we shall apply the general formalism of Section 3 by obtaining and evaluating series representations of various limiting forms of the H_n and illustrating how such information is used to compute bounds on effective properties of porous and other composite media. We begin by briefly describing bounds on effective properties. This is followed by some specific results for models of fully penetrable spheres ($\lambda = 0$), totally impenetrable spheres ($\lambda = 1$), and spheres distributed with arbitrary λ.

4.1. Bounds on Transport Properties

Doi's upper bound on the fluid permeability k of an isotropic porous medium is given by

$$k \leqslant \frac{2}{3} \int_0^\infty x\, dx \left[F_{\mathrm{mm}}(x) - \frac{2\phi}{s} F_{\mathrm{sm}}(x) + \frac{\phi^2}{s^2} F_{\mathrm{ss}}(x) \right] \tag{4.6}$$

where it is to be recalled that ϕ and s are the porosity and specific surface, respectively. Doi actually referred to the matrix phase as the void phase. (Note that for statistically isotropic media, the two-point functions depend only upon the relative distance x between the two points.) In Doi's language the correlation function F_{mm} is simply what we have been referring to as S_2. Doi has suggested a means of obtaining an infinite hierarchy of bounds on k from the variational procedure he employs. For example, the next bound in the hierarchy involves not only one-point (ϕ, s) and two-point $(F_{\text{mm}}, F_{\text{sm}}, F_{\text{ss}})$ information, but three-point information $(F_{\text{mmm}}, F_{\text{smm}}, F_{\text{ssm}}, F_{\text{sss}})$.

It is instructive to express explicitly the two-point quantities that arise in Doi's bounds in terms of the ρ_n, which, in principle, are known quantities for the ensemble under consideration. Using the Mayer representation of the H_n, Eqs. (3.16), (3.18), and (3.19), combined with Eqs. (4.1), (4.3), and (4.4), we have for a system of (possibly overlapping) spheres

$$F_{\text{mm}}(\mathbf{x}_1, \mathbf{x}_2) = \sum_{s=0}^{\infty} \frac{(-1)^s}{s!} \int \rho_s(\mathbf{r}^s) \prod_{j=1}^{s} m^{(2)}(\mathbf{x}_1, \mathbf{x}_2; \mathbf{r}_j)\, d\mathbf{r}_j \Bigg|_{a_1 = a_2 = R} \tag{4.7}$$

$$F_{\text{sm}}(\mathbf{x}_1, \mathbf{x}_2) = -\frac{\partial}{\partial a_1} \Bigg[\sum_{s=0}^{\infty} \frac{(-1)^s}{s!} \times \int \rho_s(\mathbf{r}^s) \prod_{j=1}^{s} m^{(2)}(\mathbf{x}_1, \mathbf{x}_2; \mathbf{r}_j)\, d\mathbf{r}_j \Bigg]_{a_1 = a_2 = R} \tag{4.8}$$

and

$$F_{\text{ss}}(\mathbf{x}_1, \mathbf{x}_2) = \frac{\partial}{\partial a_1} \frac{\partial}{\partial a_2} \Bigg[\sum_{s=0}^{\infty} \frac{(-1)^s}{s!} \times \int \rho_s(\mathbf{r}^s) \prod_{j=1}^{s} m^{(2)}(\mathbf{x}_1, \mathbf{x}_2; \mathbf{r}_j)\, d\mathbf{r}_j \Bigg]_{a_1 = a_2 = R} \tag{4.9}$$

Representation (4.7) for F_{mm} was first derived by Torquato and Stell.(11) However, representations (4.8) for F_{sm} and (4.9) for F_{ss} are new and hence provide a means of calculating them and the Doi bound on k for the first time for a system of spheres distributed with arbitrary degree of impenetrability.

The Weissberg–Prager(18) upper bound on k was derived using a variational principle different than the one employed by Doi, and, as a result, the statistical quantities that arise in the former (ϕ, s, $G_1^{(1)} = G_2$, $G_2^{(1)} = G_3$) and a quantity closely related to F_{sp} (described in footnote 2) are, in general, different than those that arise in the latter. The Weissberg–Prager variational principle can also be extended to yield an infinite hierarchy of bounds that involve generalizations of the statistical quantitites that are involved in the Weissberg–Prager bound. A natural question which comes to mind is: What is the connection between the Doi and the Weissberg–Prager hierarchy of bounds on k? Obviously, in order to answer this question, one must quantitatively understand the relationship between the two different sets of statistical quantities that arise in the bounds. Such an understanding is provided by the general formalism described in Section 3.

In what follows it will be useful to express explicitly the series representations of the $G_q^{(1)}$ and of F_{sp}. Combination of Eqs. (3.16), (3.18), and (3.19) together with Eqs. (4.2) and (4.5) gives

$$G_q^{(1)}(\mathbf{x}_1; \mathbf{r}^q) = \prod_{l=1}^{q} e(y_{1l}; a_1) \sum_{s=0}^{\infty} \frac{(-1)^s}{s!} \times \int \rho_{q+s}(\mathbf{r}^{q+s}) \prod_{j=q+1}^{q+s} m(y_{1j}; a_1)\, d\mathbf{r}_j \Bigg|_{a_1=R} \tag{4.10}$$

and

$$F_{\text{sp}}(\mathbf{x}_1, \mathbf{r}_2) = -\frac{\partial}{\partial a_1}\left[e(y_{11}; a_1) \sum_{s=0}^{\infty} \frac{(-1)^s}{s!} \times \int \rho_{1+s}(\mathbf{r}^{1+s}) \prod_{j=2}^{1+s} m(y_{1j}; a_1)\, d\mathbf{r}_j \right]_{a_1=R} \tag{4.11}$$

Representation (4.10) was first obtained by Torquato.$^{(16)}$ Representation (4.11) for $F_{\text{sp}}(\mathbf{x}_1, \mathbf{r}_2)$ is new, however. Recall that the latter gives the correlation associated with finding a point at $\mathbf{x}_1$ on the two-phase interface and a sphere center at $\mathbf{r}_2$.

Torquato$^{(16)}$ has recently derived first-order cluster bounds on the effective conductivity σ_e of media composed of equisized, partially penetrable spheres of conductivity σ_2 distributed through a matrix of conductivity σ_1:

$$\left[\left\langle\frac{1}{\sigma}\right\rangle - \frac{\phi^2\eta^2(1/\sigma_2 - 1/\sigma_1)^2}{A_1/\sigma_1 + B_1(1/\sigma_2 - 1/\sigma_1)}\right]^{-1} \leqslant \sigma_e \leqslant \left[\langle\sigma\rangle - \frac{\phi^2\eta^2(\sigma_2-\sigma_1)^2}{A_2\sigma_1 + B_2(\sigma_2-\sigma_1)}\right] \tag{4.12}$$

Here the $A_i = A_i[\phi, \rho_2]$ and $B_i = B_i[\phi, G_1^{(1)}, G_2^{(1)}]$ are integrals that involve the statistical quantities given within the brackets, and $\eta = \rho 4\pi R^3/3$, where R is the radius of a sphere. Torquato$^{(16)}$ also derived nth-order cluster bounds on σ_e which depend upon the sets $\rho_1, \rho_2, \ldots, \rho_{2n}$ and $G_0^{(1)}$ $(=\phi)$, $G_1^{(1)}, \ldots, G_{2n}^{(1)}$. It should be noted that the cluster bounds are the conduction analogue of the Weissberg–Prager-type bounds on k. Beran$^{(2)}$ has derived a different set of bounds on σ_e, which is applicable to general two-phase media:

$$\left[\left\langle\frac{1}{\sigma}\right\rangle - \frac{\phi^2(1-\phi)^2(1/\sigma_2 - 1/\sigma_1)^2}{C_1/\sigma_1 + D_1(1/\sigma_2 - 1/\sigma_1)}\right]^{-1} \leqslant \sigma_e \leqslant \left[\langle\sigma\rangle - \frac{\phi^2(1-\phi)^2(\sigma_2-\sigma_1)^2}{C_2\sigma_1 + D_2(\sigma_2-\sigma_1)}\right] \tag{4.13}$$

Here the $C_i = C_i[S_1, S_2]$ and $D_i = D_i[S_1, S_2, S_3]$. Although the Beran and Torquato bounds have a similar form, they involve different statistical quantities. Are the Beran and Torquato bounds ever equal to one another? Such a question can only be answered by establishing the connection between the $G_n^{(1)}$ and the S_n using the formalism of Section 3. The answer to this question is discussed in Section 4.3.

4.2. Results for Fully Penetrable Spheres

The Mayer representation of the n-point distribution functions is the most natural one to use when it is desired to calculate them exactly. Consider the evaluation of G_n and H_n for a mixture of p solute particles of radii $b_1,..., b_p$, respectively, and N solvent particles that are fully penetrable to one another (i.e., spatially uncorrelated). For such a system, we have

$$\rho_n(\mathbf{r}^n) \to \rho^n \tag{4.14}$$

Upon use of Eq. (3.15), we find

$$\begin{aligned}\frac{G_n(\mathbf{x}^p; \mathbf{r}^q)}{\prod_{l=1}^{q} \prod_{k=1}^{p} e(y_{kl}; a_k)} &= \rho^q - \rho^{q+1} V_p(\mathbf{x}^p) + \frac{\rho^{q+2}}{2!} V_p^2(\mathbf{x}^p) - \cdots \\ &= \rho^q \exp[-\rho V_p(\mathbf{x}^p)], \qquad n = p+q \end{aligned} \tag{4.15}$$

where

$V_p(\mathbf{x}^p)$ = Union volume of p spheres of radii $a_1,..., a_p$, respectively, centered at $\mathbf{x}_1,..., \mathbf{x}_p$, respectively (where it is to be recalled that $a_i = R + b_i$ for $b_i > 0$ and $a_i = R - c_i$ for $b_i = 0$; a_i being the minimum separation distance between solute and solvent centers) (4.16)

For the case of point solute particles with $a_i = R$ and $p = 1$, Eq. (4.15) reduces to the point/$(n-1)$-particle distribution function for fully penetrable spheres derived by Torquato.(16) In the instance of point solute particles with $a_i = R$, $i = 1,..., p$, and $q = 0$, Eq. (4.15) is identical to the n-point matrix probability function S_n for fully penetrable spheres derived by Torquato and Stell.(14)

In general, for this model, the n-point distribution function associated with finding the centers of m solute particles of radii $b_1,..., b_m$ at $\mathbf{x}^m$ on the surfaces $\mathscr{S}_1,..., \mathscr{S}_m$, respectively, $p - m$ of the solute centers of radii

$b_{m+1},\ldots, b_p$ at $\mathbf{x}^{p-m}$ in $D_{m+1},\ldots, D_p$, respectively, and q solvent centers of radius R at $\mathbf{r}^q$ is given by

$$H_n(\mathbf{x}^m; \mathbf{x}^{p-m}; \mathbf{r}^q)$$

$$= (-1)^m \rho^q \exp[-\rho V_p(\mathbf{x}^p)] \frac{\partial}{\partial a_1} \cdots \frac{\partial}{\partial a_m} \prod_{l=1}^{q} \prod_{k=1}^{p} e(y_{kl}; a_k)$$

$$+ (-1)^m \rho^q \prod_{l=1}^{q} \prod_{k=1}^{p} e(y_{kl}; a_k) \frac{\partial}{\partial a_1} \cdots \frac{\partial}{\partial a_m} \exp[-\rho V_p(\mathbf{x}^p)] \tag{4.17}$$

Here we have made use of Eqs. (2.9a) and (4.15). For $q=0$ the first term of Eq. (4.17) is identically zero.

As a simple application of (4.17), consider obtaining the distribution function associated with finding a point at $\mathbf{x}_1$ on the matrix–particle interface and the center of a sphere of radius R at $\mathbf{r}_1$ for a system of fully penetrable spheres. From Eqs. (4.5) and (4.17), we find

$$\begin{aligned} F_{\mathrm{sp}}(\mathbf{x}_1, \mathbf{r}_1) &= \rho\delta(y_{11} - a_1) \exp(-\rho 4\pi R^3/3) \\ &\quad + \rho^2 4\pi R^2 \exp(-\rho 4\pi R^3/3)\, e(y_{11}; R) \\ &= \rho\delta(y_{11} - a_1)\phi + \rho s e(y_{11}; R) \end{aligned} \tag{4.18}$$

where $\phi = \exp(-\rho 4\pi R^3/3)$ is the matrix volume fraction and $s = 4\pi R^2 \rho\phi$ is the specific surface for the model.(18,25) Note that the first term of Eq. (4.18) is zero everywhere except when $\mathbf{x}_1$ is on the surface of the sphere centered at $\mathbf{r}_1$ (i.e., when $y_{11} = |\mathbf{x}_1 - \mathbf{r}_1| = R$). The second term in (4.18) is the contribution to F_{sp} when $\mathbf{x}_1$ and $\mathbf{r}_1$ describe positions on different spheres. When $y_{11} \to \infty$, Eq. (4.18) states that $F_{\mathrm{sp}} \to \rho s$, as expected [cf. Eq. (2.11)].

4.3. Results for Totally Impenetrable Spheres

Consider a statistically isotropic distribution of totally impenetrable spheres ($\lambda = 1$) of equal radius R. For such a model, we obtain some new results for the two-point surface correlation functions F_{sm}, F_{ss}, and F_{sp}. Using Eqs. (4.8), (4.9), and (4.11) and the fact that, for impenetrable spheres, the series are truncated after two-body terms (cf. Section 3), we have

$$F_{\mathrm{sm}}(x) = s - \rho\delta \otimes m - \bar{F}_{\mathrm{sm}}(x) \tag{4.19}$$

$$F_{\mathrm{ss}}(x) = \rho\delta \otimes \delta + \bar{F}_{\mathrm{ss}}(x) \tag{4.20}$$

$$F_{\mathrm{sp}}(x) = \delta(x - R)(\rho - \rho_2 \otimes m) + \bar{F}_{\mathrm{sp}}(x) \tag{4.21}$$

where $\delta(x-R)$ is the Dirac delta function, m is the step function defined by Eq. (2.5) with $a_i = R$, and $f \otimes h$ denotes the three-dimensional convolution integral

$$\int f(x)\, h(|\mathbf{x}-\mathbf{x}'|)\, d\mathbf{x}'$$

for any pair of functions f and h. The terms with overbars in (4.19)–(4.21) are also convolution integrals:

$$\bar{F}_{\text{sm}}(x) = \rho_2 \otimes \delta \otimes m \tag{4.22}$$

$$\bar{F}_{\text{ss}}(x) = \rho_2 \otimes \delta \otimes \delta \tag{4.23}$$

$$\bar{F}_{\text{sp}}(x) = e(r;\, R)\, \rho_2 \otimes \delta \tag{4.24}$$

Clearly, $\bar{F}_{\text{sm}}$ and $\bar{F}_{\text{ss}}$ can each be expressed in terms of $\bar{F}_{\text{sp}}$, i.e.,

$$\bar{F}_{\text{sm}}(x) = [\bar{F}_{\text{sp}}/e] \otimes m \tag{4.25}$$

and

$$\bar{F}_{\text{ss}}(x) = [\bar{F}_{\text{sp}}/e] \otimes \delta \tag{4.26}$$

To our knowledge, relations (4.25) and (4.26) are new.

Having established that all of the correlation functions can be expressed in terms of convolution integrals, we can exploit the useful property that the Fourier transform of a convolution integral is simply the product of the Fourier transforms of the individual functions. By taking the inverse Fourier transform of the transformed convolution integrals, one can reduce all of the integrals [including the sixfold integrals (4.22) and (4.23)] to one-dimensional quadratures.

The single convolution integrals in (4.19) and (4.20) are easily evaluated. We have

$$\rho\delta \otimes m = \begin{cases} \frac{1}{2}s(1 - x/2R), & x \leqslant 2R \\ 0, & x > 2R \end{cases} \tag{4.27}$$

and

$$\rho\delta \otimes \delta = \begin{cases} s/2x, & 0 < x \leqslant 2R \\ 0, & x > 2R \end{cases} \tag{4.28}$$

Note that the first term of (4.21) is nonzero only when $x = R$ and hence one only needs to know the value of the quantity $\rho - \rho_2 \otimes m$ at this single value, which is simply equal to ρ.

In order to evaluate (4.19)–(4.21), we must know the two-particle probability density function ρ_2. This quantity can be obtained for an equilibrium distribution of impenetrable spheres using the highly accurate Verlet–Weis(31) modification of the analytical Percus–Yevick expression for ρ_2.(32) Elsewhere,(33) we calculate $\bar{F}_{sm}$, $\bar{F}_{ss}$, and $\bar{F}_{sp}$ for such a distribution, using standard Fourier transform techniques,(15) for sphere volume fractions up to 94% of the random-close-packing value.(34) (Note that for this model the particle-phase volume fraction ϕ_p is simply equal to the reduced density $\eta = \rho 4\pi R^3/3 = 1 - \phi$.) Thermodynamic consistency checks (on the Verlet–Weiss pressure and compressibility) ensure highly accurate results for $\bar{F}_{sm}$, $\bar{F}_{ss}$, and $\bar{F}_{sp}$. This work(33) gives the first theoretical determinations of the two-point surface correlation functions. Figure 3 gives these quantities, scaled by their long-range values, as a function of the distance x at $\eta = 0.5$. The reason why $\bar{F}_{sp}$ has a cusp at $x = 3R$ is explained in detail in Ref. 33.

Bounds on the permeability that utilize such information were not calculated in Ref. 33, however, since the focus there was on microstructure characterization rather than on bounds that utilize this information. Here we carry out such a calculation for the Doi upper bound on k, Eq. (4.6), employing the impenetrable-sphere results for F_{mm},(15) and the surface correlation functions F_{sm} and F_{ss}.(33) The one-dimensional integral (4.6) is

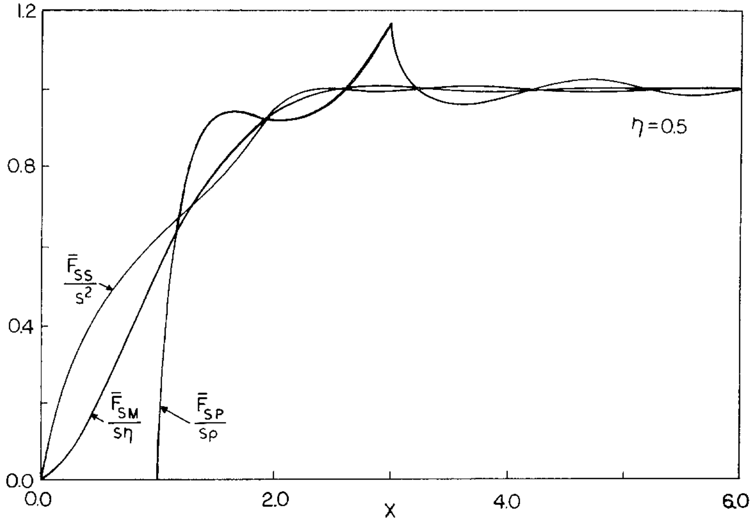

Fig. 3. The scaled two-point surface correlation functions $\bar{F}_{sm}/s\eta$, $\bar{F}_{ss}/s^2$, and $\bar{F}_{sp}/\rho s$ for impenetrable spheres of unit radius at a sphere volume fraction $\eta = 1 - \phi = 0.5$, as a function of the distance between the two points x.(33)

computed using a trapezoidal rule for $0 \leqslant \eta \leqslant 0.6$. Table I summarizes these results by giving the lower bound on k_s/k as a function of η, where

$$k_s = 2R^2/9\phi_p \tag{4.29}$$

is the exact result for Stokes flow through a very dilute assemblage of spheres. Our results reported in Table I are accurate up to the number of significant figures displayed. Berryman(19) has computed the Doi integral (4.6) using a Monte Carlo integration technique. His results are also given in Table I. Note that the discrepancies between the present results and Berryman's results increase significantly as η increases. Berryman has commented on the inaccuracies associated with his calculations, but, in light of the fact that our results have been obtained using essentially exact analytical expressions for ρ_2, we believe that he has grossly underestimated the errors involved in his technique. This Monte Carlo integration procedure is clearly not efficient when dealing with integrands that involve discontinuous functions. Figure 3 combined with (4.27) and (4.28) shows that F_{ss} is discontinuous at $x = 2R$ and that F_{sm} has a discontinuous first derivative at $x = 2R$. $F_{mm} = S_2$ is, on the other hand, much smoother and hence should contribute the smallest error to the total integral (4.6) when the Monte Carlo procedure is employed.

Table I. Comparison of the Doi Lower Bound on k_s/k, for an Assemblage of Impenetrable Spheres, as a Function of the Sphere Volume Fraction $\eta = 1 - \phi$ as Calculated in the Present Work and in Ref. 19, Respectively

	k_s/k	
η	Present work	Ref. 19
0.001	1.005	1.000
0.06	1.35	1.00
0.10	1.64	—
0.19	2.58	1.01
0.20	2.71	—
0.30	4.57	—
0.38	7.13	1.20
0.40	8.02	—
0.45	10.9	1.31
0.49	14.2	1.37
0.50	15.2	—
0.60	34.5	—

In Fig. 4 we compare our results for k_s/k to the Kozeny–Carman empirical formula

$$\frac{k_s}{k}=\frac{10\phi_p}{(1-\phi_p)^3} \tag{4.30}$$

It is clear that the Doi bounds are much more accurate than Berryman originally thought. This result has important implications, since it offers hope that bounds that incorporate the next level of microstructural information (i.e., three-point information) will lead to accurate estimates of k. Examples of such bounds are extensions of Doi's bounds described above and the Weissberg–Prager bound[18] (see Section 4.4).

As a last example for impenetrable-sphere systems, we comment on the relationship between the bounds on σ_e due to Beran,[2] Eq. (4.13), and to Torquato,[16] Eq. (4.12). Recently, Beasley and Torquato[35] have

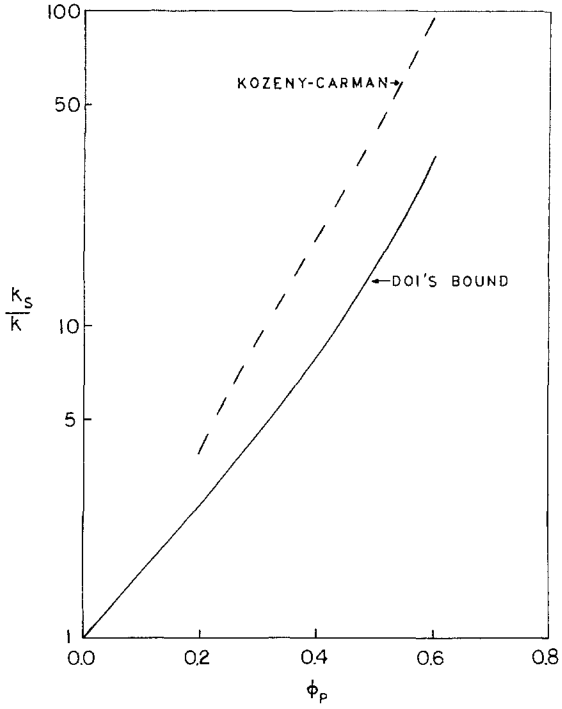

Fig. 4. Comparison of the Doi lower bound on k_s/k for impenetrable spheres computed in the present work using Eq. (4.6) and the Kozeny–Carman empirical formula (4.30) as a function of the sphere volume fraction $\eta=\phi_p=1-\phi$. Since the latter expression breaks down at large porosities, it is plotted for $\eta \geq 0.2$.

applied the formalism of the previous section to show that the Beran and Torquato bounds are identical for the special case of totally impenetrable spheres in a matrix. Using Eqs. (4.1) and (4.10) and the results of Section 3, it is easy to show that the S_n (involved in the Beran bounds) and the $G_n^{(1)}$ (involved in the Torquato bounds) are related to one another for this model. In particular, the lower order relations are given exactly by

$$S_1 = G_0^{(1)} = \phi \tag{4.31}$$

$$S_2(x_{12}) = S_1 - \int d\mathbf{r}_2\, m(|\mathbf{x}_1 - \mathbf{r}_2|)\, G_1^{(1)}(|\mathbf{x}_2 - \mathbf{r}_2|) \tag{4.32}$$

and

$$\begin{aligned} S_3(\mathbf{x}_{12}, \mathbf{x}_{13}) = S_2(x_{23}) &- \int d\mathbf{r}_3\, m(|\mathbf{x}_1 - \mathbf{r}_3|)\, e(|\mathbf{x}_2 - \mathbf{r}_3|)\, G_1^{(1)}(|\mathbf{x}_3 - \mathbf{r}_3|) \\ &+ \iint d\mathbf{r}_3\, d\mathbf{r}_4\, m(|\mathbf{x}_1 - \mathbf{r}_3|)\, m(|\mathbf{x}_2 - \mathbf{r}_4|) \\ &\times G_2^{(1)}(\mathbf{x}_3 - \mathbf{r}_3, \mathbf{x}_3 - \mathbf{r}_4) \end{aligned} \tag{4.33}$$

where $a_i = R$ in the step functions m and e, and where $\mathbf{x}_{ij} = \mathbf{x}_i - \mathbf{x}_j$ and $x_{ij} = |\mathbf{x}_{ij}|$. Substituting Eqs. (4.31)–(4.33) into the Beran bounds and simplifying the resulting integrals leads to the fact that the Beran and Torquato bounds are identical to one another for impenetrable-sphere models. For $\lambda < 1$, the Beran bounds prove to be slightly more restrictive than the Torquato bounds. The Beran or, equivalently, the Torquato bounds have recently been computed for an equilibrium distribution of impenetrable spheres.(36)

4.4. Results for Partially Penetrable Spheres

Here we consider results for dilute dispersions of spheres distributed with arbitrary degree of impenetrability λ. Specifically, we present new results for the Weissberg–Prager(18) inverse permeability k^{-1}, expanded through second order in the sphere volume fraction ϕ_p, in the PS(23) and PCS(24) models. In order to accomplish this, we must obtain the low-density expansions of the statistical quantities involved in the bound ($G_1^{(1)}$, $G_2^{(1)}$, and F_{sp}) for these interpenetrable-sphere models, utilizing Eqs. (4.10) and (4.11). Upon substitution of these expansions into the Weissberg–Prager lower bound on the inverse permeability k^{-1}, we find

$$k_s/k \geqslant 1 + K^{(1)}\phi_p + O(\phi_p^2) \tag{4.34}$$

where in the PS and PCS models, respectively,

$$K^{(1)} = \frac{3}{2} + \lambda\left(3 \ln 3 + \frac{143}{162}\right) \tag{4.35}$$

and

$$K^{(1)}=\frac{3}{2}-\lambda^6+\frac{11}{4}\lambda^4+\frac{5}{16}\lambda^2-\frac{9}{8}\lambda-\frac{\lambda(1+7\lambda)}{16(2\lambda+1)^2}$$
$$+\frac{\lambda}{16(2\lambda+1)^4}+\frac{3}{4}(1+3\lambda^2)\ln(2\lambda+1) \qquad (4.36)$$

The details of these calculations are described elsewhere.[37] In the extreme limits, we have that

$$K^{(1)}=3/2 \qquad (4.37)$$

for fully penetrable spheres ($\lambda=0$) and

$$K^{(1)}=3\ln 3+193/81\approx 5.68 \qquad (4.38)$$

for totally impenetrable spheres ($\lambda=1$).

There are two comments we would like to make regarding Eqs. (4.34)–(4.36). Firstly, in order to obtain exactly the permeability for arbitrary λ, the solution to the two-sphere boundary-value problem for two interpenetrating spheres must be known. Short of obtaining the solution to this nontrivial problem, low-density bounds on k offer the next best means of studying the effect of particle overlap on k. At the same ϕ_p, the results (4.34)–(4.36) generally indicate that the effect of decreasing λ is to decrease k^{-1} or increase the permeability. (For example, $K^{(1)}$ for $\lambda=1$ is almost four times larger than its counterpart for $\lambda=0$.) Secondly, when we exactly evaluate the first-order coefficient $K^{(1)}$ of the Doi bound for the case $\lambda=1$, we find that $K^{(1)}=5.0$, which is obviously less than the Weissberg–Prager value of 5.68. In other words, the Weissberg–Prager bound, through this order in ϕ_p, is sharper than the Doi bound for the case of impenetrable spheres. This is not surprising, since the former involve not only one- and two-point information (as does the latter), but also three-point information. In light of this, it is expected that the Weissberg–Prager bound will yield the most accurate bound on k for an assemblage of impenetrable spheres, through all orders in ϕ_p.

ACKNOWLEDGMENTS

The author is grateful to G. Stell for making a critical observation. I am also grateful to the referees for suggestions that clarified and enhanced the presentation and to J. D. Beasley for help with some of the computations. This work was supported in part by the Office of Basic Energy Sciences, U. S. Department of Energy, and by the Donors of the Petroleum Research Fund administered by the American Chemical Society.

REFERENCES

1. W. F. Brown, *J. Chem. Phys.* **23**:1514 (1955).
2. M. Beran, *Nuovo Cimento* **38**:771 (1965).
3. G. W. Milton, *J. Appl. Phys.* **52**:5294 (1981).
4. S. Torquato, *J. Appl. Phys.* **58**:3790 (1985).
5. S. Prager, *Phys. Fluids* **4**:1477 (1961).
6. J. G. Berryman and G. W. Milton, *J. Chem. Phys.* **83**:754 (1985).
7. R. A. Reck and S. Prager, *J. Chem. Phys.* **42**:3027 (1965).
8. M. Beran and J. Molyneux, *Q. Appl. Math.* **24**:107 (1965).
9. J. J. McCoy, *Recent Advances in Engineering 5* (Gordon and Breach, New York, 1970).
10. G. W. Milton and N. Phan-Thien, *Proc. R. Soc. Lond. A* **380**:305 (1982).
11. S. Torquato and G. Stell, *J. Chem. Phys.* **77**:2071 (1982).
12. S. Torquato and G. Stell, *J. Chem. Phys.* **78**:3262 (1983).
13. H. L. Weissberg, *J. Appl. Phys.* **34**:2636 (1963).
14. S. Torquato and G. Stell, *J. Chem. Phys.* **79**:1505 (1983).
15. S. Torquato and G. Stell, *J. Chem. Phys.* **82**:980 (1985).
16. S. Torquato, *J. Chem. Phys.* **84**:6345 (1986).
17. M. Doi, *J. Phys. Soc. Japan* **40**:567 (1976).
18. H. L. Weissberg and S. Prager, *Phys. Fluids* **13**:2958 (1970).
19. J. G. Berryman, *J. Comput. Phys.* **52**:142 (1983).
20. J. G. Kirkwood and Z. W. Salsburg, *Disc. Faraday Soc.* **15**:28 (1953).
21. J. E. Mayer and E. Montroll, *J. Chem. Phys.* **9**:2 (1941).
22. H. Reiss, H. L. Frisch, and J. L. Lebowitz, *J. Chem. Phys.* **31**:369 (1959).
23. L. Blum and G. Stell, *J. Chem. Phys.* **71**:42 (1979); **72**:2212 (1980); J. J. Salacuse and G. Stell, *J. Chem. Phys.* **77**:3714 (1982).
24. S. Torquato, *J. Chem. Phys.* **81**:5079 (1984).
25. S. Torquato and G. Stell, *J. Chem. Phys.* **80**:878 (1984).
26. Y. C. Chiew and E. D. Glandt, *J. Colloid Interface Sci.* **99**:86 (1984).
27. S. Baer and J. L. Lebowitz, *J. Chem. Phys.* **40**:3474 (1964).
28. J. E. Mayer, *J. Chem. Phys.* **15**:187 (1947).
29. P. A. Rikvold and G. Stell, *J. Chem. Phys.* **82**:1014 (1985).
30. W. W. Yau, J. J. Kirkland, and D. D. Bly, *Modern Size-Exclusion Liquid Chromatography* (Wiley-Interscience, New York, 1979).
31. L. Verlet and J. J. Weis, *Phys. Rev. A* **5**:939 (1972).
32. J. P. Hansen and I. R. McDonald, *Theory of Simple Liquids* (Academic Press, New York, 1976).
33. S. Torquato, *J. Chem. Phys.* **85**:4622 (1986).
34. J. G. Berryman, *Phys. Rev. A* **27**:1053 (1983).
35. J. D. Beasley and S. Torquato, *J. Appl. Phys.* **60**:3576 (1986).
36. S. Torquato and F. Lado, *Phys. Rev. B* **33**:6248 (1986).
37. S. Torquato and J. D. Beasley, *Phys. Fluids*, in press.